

Crystal field splitting and optical bandgap of hexagonal LuFeO₃ films

Wenbin Wang, Hongwei Wang, Xiaoying Xu, Leyi Zhu, Lixin He, Elizabeth Wills, Xuemei Cheng, David J. Keavney, Jian Shen, Xifan Wu, and Xiaoshan Xu

Citation: *Applied Physics Letters* **101**, 241907 (2012); doi: 10.1063/1.4771601

View online: <http://dx.doi.org/10.1063/1.4771601>

View Table of Contents: <http://scitation.aip.org/content/aip/journal/apl/101/24?ver=pdfcov>

Published by the AIP Publishing

Articles you may be interested in

Band gap narrowing of ZnO:N films by varying rf sputtering power in O₂/N₂ mixtures

J. Vac. Sci. Technol. B **25**, L23 (2007); 10.1116/1.2746053

Blue photoluminescence of -Ga₂S₃ and -Ga₂S₃:Fe²⁺ single crystals

Appl. Phys. Lett. **83**, 1947 (2003); 10.1063/1.1609254

Manifestation of quasi-symmetry of the cation sites of Gd₂SiO₅, Y₂SiO₅, and Lu₂SiO₅ in the spectra of the impurity ion Pr³⁺

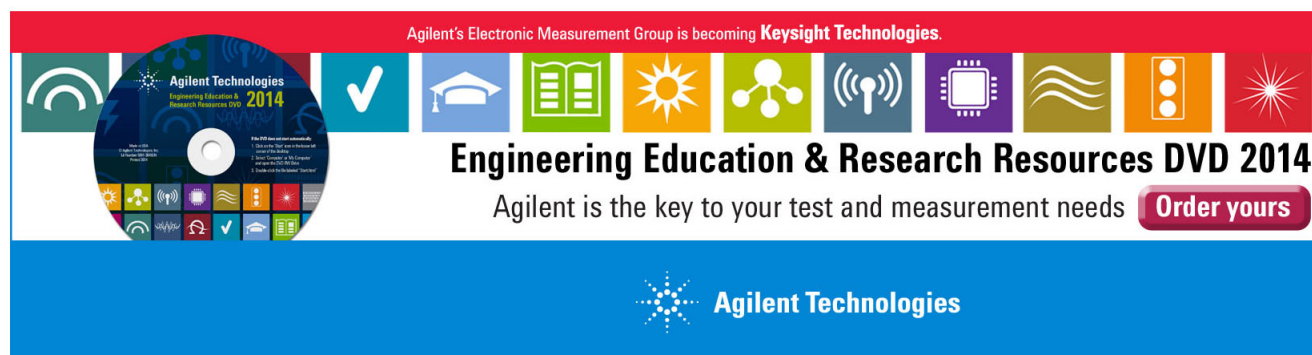
Low Temp. Phys. **27**, 574 (2001); 10.1063/1.1388423

Influence of the chemical environment on the electronic structure and spectroscopic properties of Er³⁺ doped Cs₃Lu₂Cl₉, Cs₃Lu₂Br₉, and Cs₃Y₂I₉

J. Chem. Phys. **110**, 12033 (1999); 10.1063/1.479139

Crystal-field splitting, magnetic interaction, and vibronic excitations of 244 Cm³⁺ in YPO₄ and LuPO₄

J. Chem. Phys. **109**, 6800 (1998); 10.1063/1.477326

The advertisement features a red header with the text 'Agilent's Electronic Measurement Group is becoming Keysight Technologies.' Below this is a row of icons representing various engineering and research fields. The central focus is a DVD labeled 'Agilent Technologies Engineering Education & Research Resources DVD 2014'. To the right of the DVD, the text 'Engineering Education & Research Resources DVD 2014' is displayed in a large, bold font. Below this, the slogan 'Agilent is the key to your test and measurement needs' is shown, followed by a red button with the text 'Order yours'. The bottom of the advertisement is a blue banner with the Agilent Technologies logo and name.

Crystal field splitting and optical bandgap of hexagonal LuFeO₃ films

Wenbin Wang,^{1,2} Hongwei Wang,^{3,4} Xiaoying Xu,² Leyi Zhu,⁵ Lixin He,⁴ Elizabeth Wills,⁶ Xuemei Cheng,⁶ David J. Keavney,⁷ Jian Shen,^{1,8} Xifan Wu,^{3,a)} and Xiaoshan Xu^{2,a)}

¹Department of Physics, University of Tennessee, Knoxville, Tennessee 37996, USA

²Materials Science and Technology Division, Oak Ridge National Laboratory, Oak Ridge, Tennessee 37831, USA

³Department of Physics and Institute for Computational Molecular Science, Temple University, Philadelphia, Pennsylvania 19122, USA

⁴Key Laboratory of Quantum Information, University of Science and Technology of China, Hefei, Anhui 230026, China

⁵Materials Science Division, Argonne National Laboratory, Argonne, Illinois 60439, USA

⁶Department of Physics, Bryn Mawr College, Bryn Mawr, Pennsylvania 19010, USA

⁷Advanced Photon Source, Argonne National Laboratory, Argonne, Illinois 60439, USA

⁸Department of Physics, Fudan University, Shanghai 200433, China

(Received 1 October 2012; accepted 27 November 2012; published online 11 December 2012)

Hexagonal LuFeO₃ films have been studied using x-ray absorption and optical spectroscopy. The crystal splitting of Fe³⁺ is extracted as $E_{e'} - E_{e''} = 0.7$ eV and $E_{d_1'} - E_{e'} = 0.9$ eV, and a 2.0 eV optical bandgap is determined assuming a direct gap. First-principles calculations confirm the experiments that the relative energies of crystal field splitting states do follow $E_{d_1'} > E_{e'} > E_{e''}$ with slightly underestimated values and a bandgap of 1.35 eV. © 2012 American Institute of Physics. [<http://dx.doi.org/10.1063/1.4771601>]

Multiferroic materials which simultaneously exhibit more than one type of ferroic order have many advantages over other existing materials in terms of applications in sensor, actuator, and information storage and processing.^{1,2} Hexagonal ferrites (h-RFeO₃, R = Sc, Y, Ho-Lu) were recently found to be a class of multiferroic materials.^{3–10} In particular, it is suggested by experiments that h-LuFeO₃ may be both ferroelectric and antiferromagnetic at room temperature, indicating important application potential.¹⁰ It is fascinating that h-RFeO₃ exhibit distinct properties such as ferrimagnetism, abnormal magneto-dielectric couplings, and structural instability compare with RMnO₃.^{3,4,6,7} These unexpected properties are supposed to have electronic origins because h-RFeO₃ and RMnO₃ are isomorphic, and the radius of Fe³⁺ and Mn³⁺ are almost identical.^{3,4} Therefore, the information on the electronic structures is crucial in understanding the intriguing multiferroicity of h-RFeO₃.

Hexagonal RFeO₃ are not stable in free standing bulk form. They can be stabilized by quenching a levitated melt in an aerodynamic levitation furnace or in solvothermal reactions.^{4,11–13} In addition, h-RFeO₃ has also been stabilized in films using pulsed laser deposition (PLD) and metal-organic chemical vapor deposition on yttrium stabilized zirconium oxides (YSZ) and Al₂O₃ substrates.^{3,5–7,9,10} The crystallographic structures of h-RFeO₃ is isomorphic to RMnO₃ with space group $P6_3cm$ (185),^{3,4} suggesting that h-RFeO₃ are also ferroelectric, which is recently demonstrated.^{3,4,6,14} The larger spin on Fe³⁺ compared with Mn³⁺ corresponds to stronger magnetic interactions, allowing for higher magnetic ordering temperature, which has been indicated by recent experiments.^{5,6,10} In stark contrast to the large amount of work devoted to RMnO₃, detailed studies on the h-RFeO₃,

and especially of the electronic structures that are crucial for understanding the structural, ferroelectric, and magnetic properties are still lacking.^{9,15–17}

In this paper, we investigate the electronic properties of h-LuFeO₃ films using x-ray absorption and optical spectroscopy. The analysis of the x-ray absorption spectra (XAS) using crystal field theory reveal a splitting of the Fe 3d levels significantly higher than that of Fe³⁺ in LuFe₂O₄, indicating stronger Fe-O interactions. The extracted optical bandgap from optical absorption spectra (assuming a direct gap) is 2.0 ± 0.1 eV, somewhat smaller than that of perovskite ferrites.¹⁸ The experimental findings have been confirmed by our electronic structure calculations.

The XAS was studied on 50 nm h-LuFeO₃ films grown on Al₂O₃ substrates using PLD with 30 nm Pt buffer layer (Fig. 1(a)) to avoid charging effect.¹⁹ The XAS was taken at beam line 4-ID-C at the Advanced Photon Source using polarized synchrotron x-rays. A 20 nm thick h-LuFeO₃ film was grown on a YSZ substrate using PLD (Fig. 1(b)) for optical spectroscopy measurements. Part of the substrate was covered by a mask at growth, so it can be used as a reference in the optical transmittance measurements. Optical spectra were collected in transmittance mode using a Varian Cary 5000 spectrometer.

Figure 2(a) shows the XAS corresponding to transitions from a Fe $2p^6 3d^5$ to a Fe $2p^5 3d^6$ multiplet. In the spectra, two groups of peaks separated by approximately 12 eV can be distinguished. Two well-separated peaks (709.1 and 710.7 eV) are observed for the *s* polarization, while additional intensities are observed for *p* polarization as a peak at 709.8 eV, indicating a strong dichroism much more prominent than that of YMnO₃.²⁰

These spectra details are determined by dipole and spin selection rules and a combination of effects from crystal-field, spin-orbit coupling, *d-p* and *d-d* interactions and Fe 3d

^{a)}Authors to whom correspondence should be addressed: Electronic addresses: xiaoshan.xu@gatech.edu and xifanwu@temple.edu.

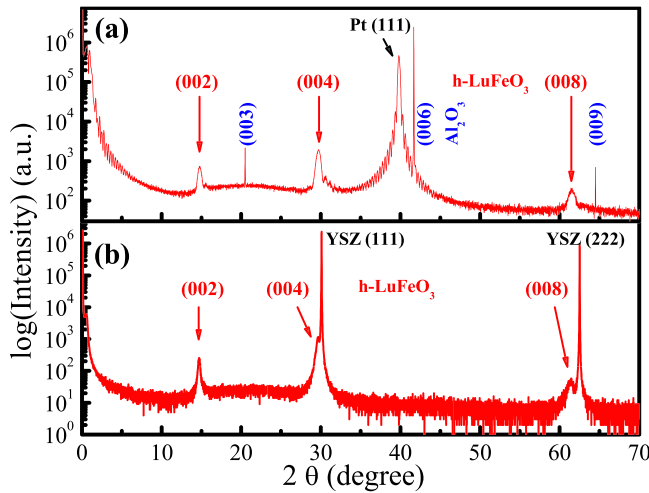


FIG. 1. The x-ray diffraction spectra of h-LuFeO₃ films grown on (a) Al₂O₃ substrates with Pt buffer layer and (b) YSZ substrates.

O 2*p* hybridization.^{21,22} In terms of one-electron energy, the Fe 2*p* states are split into 2*p*_{1/2} and 2*p*_{3/2} by the spin-orbit coupling, which has the energy scale of 15 eV, resulting in the two groups of excitations *L*₂ (2*p*_{1/2} → 3*d*) and *L*₃ (2*p*_{3/2} → 3*d*) in Fig. 2(a).^{21,23} For the Fe 3*d* states, the one-electron states are mainly split by crystal fields, which is on the order of one eV.^{21,23} Here, the trigonal-bipyramidal local environment of Fe gives rise to a symmetry that can be represented by the *D*_{3*h*} point group as a good approximation, as shown in Fig. 2(c). In this case, Fe 3*d* states split into irreducible representations (IR) *e*^{''}(*xz*, *yz*), *e*['](*xx* − *yy*, *xy*) and *a*₁['](*zz*) while Fe 2*p* orbitals can be reduced to states corresponding to IR *e*['](*x*, *y*) and *a*₂^{''}(*z*).²⁴ A recent work on LuFe₂O₄ in which Fe³⁺ sites also sit in a trigonal-bipyramidal local environment has shown that the energies of these crystal field states follow *E*_{*a*₁[']} > *E*_{*e*[']} > *E*_{*e*^{''}}.²⁵ Similar results are also found for Mn³⁺ in a *D*_{3*h*} symmetry.²⁰

The transition probability in the XAS depends on the matrix elements $|\langle \psi_i | \hat{E} \cdot \vec{r} | \psi_f \rangle|^2$, where the ψ_i and ψ_f are the

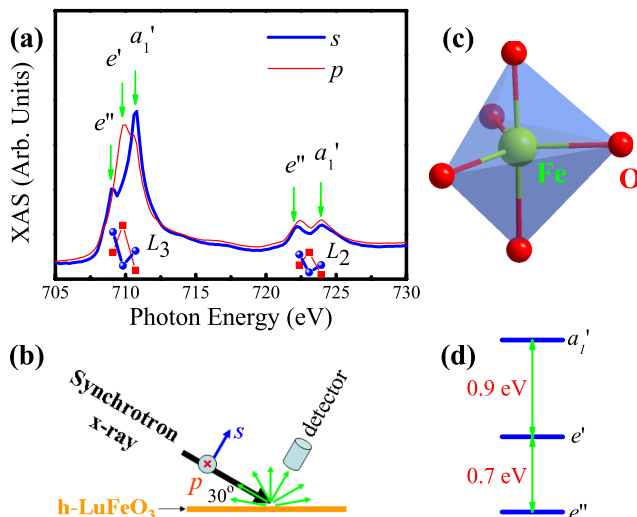


FIG. 2. Crystal field splitting of Fe sites (300K). (a) The x-ray absorption spectra corresponding to Fe 2*p* to Fe 3*d* excitations. The symbols are the calculated matrix elements from the initial to the final one-electron states. (b) Schematics of the experimental setup. (c) Schematics of the local environment of Fe sites. (d) The crystal splitting extracted from the XAS spectra.

initial and final one-electron states, \hat{E} is the direction vector of the electric field, and \vec{r} is the position vector. According to Hund's rule, the ground states of Fe³⁺ are a multiplet ⁶*A*₁['] for a 2*p*_{3/2}⁴2*p*_{1/2}²3*d*_{*e*^{''}}²3*d*_{*e*[']}²3*d*_{*a*₁[']} electronic configuration. In the ionic model that ignores hybridization between Fe 3*d* and O 2*p* state, the spin-allowed excited state multiplets and the corresponding one-electron state populations can be listed as shown in Table I.^{22,26} Since the ground state multiplet has a symmetry of *A*₁['], the dipole-allowed excited states need to contain *E*['] or *A*₂^{''} to satisfy the dipole selection rules for a *D*_{3*h*} symmetry.²⁴ The resulting dipole-allowed transitions are listed in Table I. It is clear that the photon with *z* polarization cannot excite an electron from Fe 2*p* to Fe 3*d*_{*e*[']} state. These selection rules are verified in the *L*₃ part of the XAS: for *s* polarization, the intensity in the middle is much weaker, which suggests that the three peaks at 709.1, 709.8, and 710.7 eV are coming from the effect of crystal field. As shown in Fig. 2(a) as symbols, the calculated matrix elements qualitatively agree with the dichroism for *L*₃ excitation. The less obvious agreement for *L*₂ excitations is presumably due to a mixed energy splitting from crystal field and *p*-*d* interactions.²¹ The peak positions allow for a rough determination of the crystal field splitting assuming similar *d*-*d* interactions for different Fe 3*d* states: *E*_{*e*[']} − *E*_{*e*^{''}} = 0.7 eV and *E*_{*a*₁[']} − *E*_{*e*[']} = 0.9 eV, as also shown in Fig. 2(d). The splitting is significantly larger than that in LuFe₂O₄ (*E*_{*e*[']} − *E*_{*e*^{''}} = 0.4 eV and *E*_{*a*₁[']} − *E*_{*e*[']} = 0.8 eV for Fe³⁺ sites).²⁵ The differences indicate stronger Fe-O interactions, as also suggested by the different Fe-O bond length in h-LuFeO₃ and in LuFe₂O₄.^{4,27}

In order to further elucidate the electronic structure of the h-LuFeO₃, we measured optical absorption spectra of the h-LuFeO₃ films. The observed spectra (Fig. 3) shows three peak-like features at approximately 2.3, 2.9, and 3.9 eV, consistent with the recently reported optical properties of h-RFeO₃ films.⁹ Based upon the overall intensity $\sim 10^7$ m^{−1}, these peaks correlate to dipole-allowed excitations. Since the Fe³⁺ has a 3*d*⁵ configuration, all the on-site excitations are spin forbidden. Therefore, the peak at 2.3 eV is coming from charge transfer excitations.¹⁸ A 2.0 ± 0.1 eV optical bandgap was extracted using plots of α^2 versus energy (Fig. 3 inset), assuming a direct gap.²⁸

First-principles electronic structure calculations can provide insightful picture of crystal field splitting. We determined our projected density of states (PDOS) by the density functional theory (DFT) implemented in the Vienna ab initio simulations package (VASP).^{29,30} We adopted the Perdew-Burke-Ernzerhof functional revised for solids (PBEsol)³¹ in which the spin-polarized generalized gradient approximation

TABLE I. The spin-allowed excited states and the dipole selection rules from the ⁶*A*₁['] (2*p*_{3/2}⁴2*p*_{1/2}²3*d*_{*e*^{''}}²3*d*_{*e*[']}²3*d*_{*a*₁[']}) ground state with a linearly polarized photon. Note that both 2*p*_{3/2}⁴2*p*_{1/2}² and 2*p*_{3/2}³2*p*_{1/2}² multiplets contain IR *E*['] and *A*₂^{''}.

3 <i>d</i> Configuration	IR	Allowed Polarization
3 <i>d</i> _{<i>e</i>^{''}} ³ 3 <i>d</i> _{<i>e</i>[']} ² 3 <i>d</i> _{<i>a</i>₁[']} ¹	<i>A</i> ₁ ['] + <i>A</i> ₂ ^{''} + <i>E</i> ['] + <i>E</i> ^{''}	<i>x</i> , <i>y</i> , <i>z</i>
3 <i>d</i> _{<i>e</i>[']} ² 3 <i>d</i> _{<i>e</i>^{''}} ³ 3 <i>d</i> _{<i>a</i>₁[']} ¹	<i>A</i> ₁ ['] + <i>A</i> ₂ ^{''} + <i>E</i> ['] + <i>E</i> ^{''}	<i>x</i> , <i>y</i>
3 <i>d</i> _{<i>e</i>^{''}} ² 3 <i>d</i> _{<i>e</i>[']} ² 3 <i>d</i> _{<i>a</i>₁[']} ²	<i>E</i> ['] + <i>A</i> ₂ ^{''}	<i>x</i> , <i>y</i> , <i>z</i>

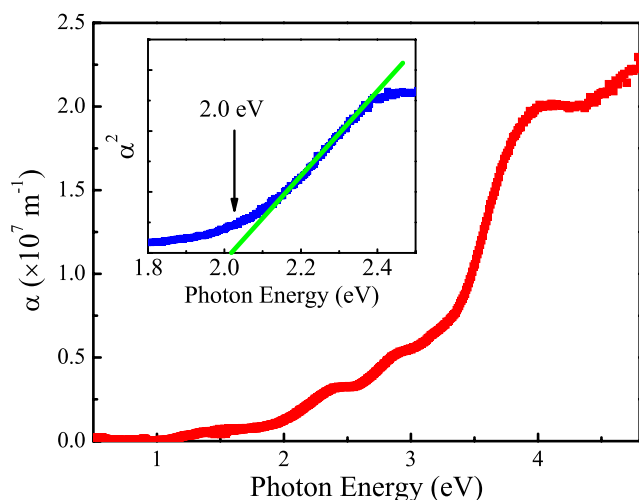


FIG. 3. Optical absorption coefficient α as a function of photon energy. Inset: α^2 as a function of photon energy, which indicates an optical bandgap of 2.0 eV.

(GGA) is made in treating the exchange correlation effect of electrons. The resulting PDOS is presented in Fig. 4. One can clearly see that our theoretical results are consistent with the experimental data in which the crystal field states follow $E_{d'_1} > E_{e'} > E_{e''}$. An unambiguous assignment of the crystal field states and energies can be further obtained by generating maximally localized Wannier functions (MLWFs)³² based on the ground state electronic structure in the selected energy window spanning all the crystal field states under consideration. The resulting MLWFs for each crystal field state are shown in Fig. 4 and the resulting energies are $E_{e'} - E_{e''} = 0.41$ eV and $E_{d'_1} - E_{e'} = 0.81$ eV, which are close to the experimental values of 0.7 and 0.9 eV, respectively. This qualitative agreement between experiment and theory is expected within the frame work of DFT. However, we should be aware that a more proper treatment of electron-hole excitations by GW based Bethe-Salpeter method^{33,34} can further improve the theoretical prediction.

To overcome the severely underestimated bandgap due to the delocalization error arising from the incomplete can-

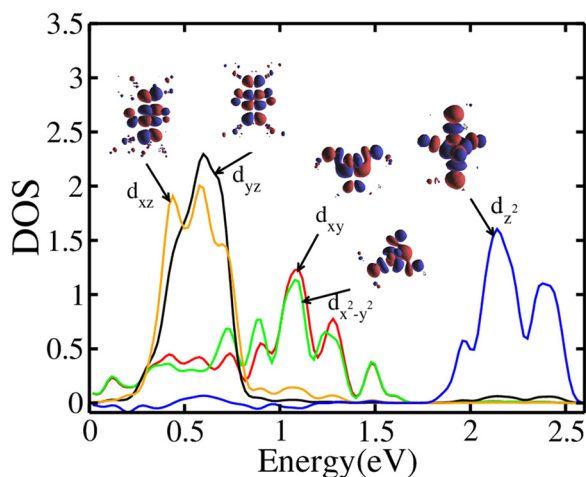


FIG. 4. Projected density of states for conduction band of h-LuFeO₃ with theoretical ground state structure (space group $P6_3cm$) and MLWFs (by WIEN2K software package (Refs. 35 and 36)) with crystal field splitting states characters.

cellation of the spurious self-interaction, we used the GGA + U with the effective U value ($U_{\text{eff}} = U - J$) of 4.61 eV.³⁷ This gives a bandgap of $E_g = 1.35$ eV, which still underestimates our experimental value.²⁸ Again, a more proper treatment of self-energy by GW method will further bring the theoretical predictions closer to the experimental value.

In conclusion, we have studied h-LuFeO₃ films using x-ray and optical spectroscopy. The strong dichroism in XAS and large crystal field energy splitting of Fe³⁺ may be related to the stability of hexagonal phase of LuFeO₃. A 2.0 eV optical bandgap originated from charge transfer excitations is determined from the optical spectra. This important information of electron structure, confirmed by DFT calculations will definitely benefit further studies of h-LuFeO₃.

Research supported by the US DOE, BES MSED (X.S.X.), and partially supported by the Chinese 973 Program Grant No. 2011CB921801 (J.S.), the US DOE BES Grant DE-SC0002136 (W.B.W.), and the NSF Grant No. 1053854 (X.M.C.). Use of the APS supported by the US DOE, BES Contract No. DE-AC02-06CH11357.

¹D. Khomskii, *Physics* 2, 20 (2009).

²N. A. Spaldin, S.-W. Cheong, and R. Ramesh, *Phys. Today* 63, 38 (2010).

³A. A. Bossak, I. E. Graboy, O. Y. Gorbenko, A. R. Kaul, M. S. Kartavseva, V. L. Svetchnikov, and H. W. Zandbergen, *Chem. Mater.* 16, 1751 (2004).

⁴E. Magome, C. Moriyoshi, Y. Kuroiwa, A. Masuno, and H. Inoue, *Jpn. J. Appl. Phys.*, 49, 09ME06 (2010).

⁵A. R. Akbashev, A. S. Semisalova, N. S. Perov, and A. R. Kaul, *Appl. Phys. Lett.* 99, 122502 (2011).

⁶Y. K. Jeong, J.-H. Lee, S.-J. Ahn, S.-W. Song, H. M. Jang, H. Choi, and J. F. Scott, *J. Am. Chem. Soc.* 134, 1450 (2012).

⁷H. Iida, T. Koizumi, Y. Uesu, K. Kohn, N. Ikeda, S. Mori, R. Haumont, R. Janolin, P. E. Kiat, J. M. Fukunaga, and Y. Noda, *J. Phys. Soc. Jpn.* 81, 024719 (2012).

⁸L. J. Downie, R. J. Goffa, W. Kockelmann, S. D. Forderc, J. E. Parkerd, F. D. Morrison, and P. Lightfoot, *J. Solid State Chem.* 190, 52 (2012).

⁹V. V. Pavlov, A. R. Akbashev, A. M. Kalashnikova, V. A. Rusakov, A. R. Kaul, M. Bayer, and R. V. Pisarev, *J. Appl. Phys.* 111, 056105 (2012).

¹⁰W. B. Wang, J. Zhao, Z. Gai, N. Balke, M. Chi, H. N. Lee, W. Tian, L. Zhu, X. Cheng, D. J. Keavney, J. Yi, T. Z. Ward, P. C. Snijders, H. M. Christen, J. Shen, and X. S. Xu, e-print arXiv 1209.3293 (2012).

¹¹K. Kuribayashi, K. Nagashio, K. Niwata, M. S. V. Kumar, and T. Hibiya, *Rev. Adv. Mater. Sci.* 18, 444 (2008).

¹²M. S. V. Kumar, K. Kuribayashi, and K. Kitazono, *J. Am. Ceram. Soc.* 92, 903 (2009).

¹³M. S. V. Kumar, K. Nagashio, T. Hibiya, and K. Kuribayashi, *J. Am. Ceram. Soc.* 91, 806 (2008).

¹⁴C. J. Fennie and K. M. Rabe, *Phys. Rev. B* 72, 100103 (2005).

¹⁵G. J. McCarthy, P. V. Gallagher, and C. Sipe, *Mater. Res. Bull.* 8, 1277-1284 (1973).

¹⁶I. E. Chupis and G. A. Smolenskii, *Sov. Phys. Usp.* 25, 475 (1982).

¹⁷R. Thomas, J. F. Scott, D. N. Bose, and R. S. Katiyar, *J. Phys: Condens. Matter* 22, 423201 (2010).

¹⁸X. S. Xu, T. V. Brinzari, S. Lee, Y. H. Chu, L. W. Martin, A. Kumar, S. McGill, R. C. Rai, R. Ramesh, V. Gopalan, S.-W. Cheong, and J. L. Musfeldt, *Phys. Rev. B* 79, 134425 (2009).

¹⁹The lattice constants of h-LuFeO₃ films on YSZ and on pt buffered Al₂O₃ are the same within the experimental uncertainty, due to the fast structural relaxation (see Ref. 3). Our measurements show similar XAS spectra for the two kinds of films, while those of h-LuFeO₃/YSZ have worse statistics due to the charging problem.

²⁰D.-Y. Cho, J.-Y. Kim, B.-G. Park, K.-J. Rho, J.-H. Park, H.-J. Noh, B. J. Kim, S.-J. Oh, H.-M. Park, J.-S. Ahn, H. Ishibashi, S.-W. Cheong, J. H. Lee, P. Murugavel, T. W. Noh, A. Tanaka, and T. Jo, *Phys. Rev. Lett.* 98, 217601 (2007).

²¹J. Stohr and H. C. Siegmann, *Magnetism from Fundamentals to Nanoscale Dynamics* (Springer, Berlin, 2006).

- ²²G. van der Laan, J. Zaanen, G. A. Sawatzky, R. Karnatak, and J.-M. Esteve, *Phys. Rev. B* **33**, 4253 (1986).
- ²³H. Wadati, D. Kobayashi, H. Kumigashira, K. Okazaki, T. Mizokawa, A. Fujimori, K. Horiba, M. Oshima, N. Hamada, M. Lippmaa, M. Kawasaki, and H. Koinuma, *Phys. Rev. B* **71**, 035108 (2005).
- ²⁴F. A. Cotton, *Chemical Applications of Group Theory* (Wiley, New York, 1990).
- ²⁵K.-T. Ko, H.-J. Noh, J.-Y. Kim, B.-G. Park, J.-H. Park, A. Tanaka, S. B. Kim, C. L. Zhang, and S.-W. Cheong, *Phys. Rev. Lett.* **103**, 207202 (2009).
- ²⁶These multiplets are divided into groups due to the *p-d* interactions, which have an energy scale of 5 eV (Ref. 21).
- ²⁷M. Isobe, N. Kimizuka, J. Iida, and S. Takekawa, *Acta Crystallogr., Sect. C* **46**, 1917 (1990).
- ²⁸Our first principle calculations show a fairly flat top for the valence band, indicating a mixture of direct and indirect nature of the bandgap. Here, we made the assumption that the part of optical absorption spectrum shown in Fig. 3 inset is related to a direct bandgap according to the strong absorption coefficient ($\sim 10^7 \text{ m}^{-1}$) above the gap. **The tail below the gap in Fig. 3 is consistent with a typical experimental artifact on film samples due to the reflections.**
- ²⁹G. Kresse and J. Hafner, *Phys. Rev. B* **47**, R558 (1993); G. Kresse and J. Furthmuller, *Phys. Rev. B* **54**, 11169 (1996).
- ³⁰A 500 eV planewave cutoff and $6 \times 6 \times 3$ *k* points mesh are used.
- ³¹J. P. Perdew, A. Ruzsinszky, G. I. Csonka, O. A. Vydrov, G. E. Scuseria, L. A. Constantin, X. L. Zhou, and K. Burke, *Phys. Rev. Lett.* **100**, 136406 (2008).
- ³²N. Marzari and D. Vanderbilt, *Phys. Rev. B* **56**, 12847 (1997).
- ³³G. Onida, L. Reining, and A. Rubio, *Rev. Mod. Phys.* **74**, 601 (2002).
- ³⁴W. Chen, X. Wu, and R. Car, *Phys. Rev. Lett.* **105**, 017802 (2010).
- ³⁵K. Schwartz and P. Blaha, *Comput. Mater. Sci.* **28**, 259 (2003).
- ³⁶The energy threshold separating the localized and nonlocalized electronic states is chosen to be -7Ry . The muffin-tin radii are 2.35 Bohr for Lu, 1.98 Bohr for Fe, and 1.65 Bohr for O. The criterion for the number of plane waves is chosen to be $R_{\text{MT}}^{\text{min}} * K^{\text{max}} = 7$, and the number of *k* points is $8 \times 8 \times 2$ for A-type antiferromagnetic calculation.
- ³⁷H. J. Xiang and M.-H. Whangbo, *Phys. Rev. Lett.* **98**, 246403 (2007).